

ChemComm

Accepted Manuscript



This is an *Accepted Manuscript*, which has been through the Royal Society of Chemistry peer review process and has been accepted for publication.

Accepted Manuscripts are published online shortly after acceptance, before technical editing, formatting and proof reading. Using this free service, authors can make their results available to the community, in citable form, before we publish the edited article. We will replace this *Accepted Manuscript* with the edited and formatted *Advance Article* as soon as it is available.

You can find more information about *Accepted Manuscripts* in the [Information for Authors](#).

Please note that technical editing may introduce minor changes to the text and/or graphics, which may alter content. The journal's standard [Terms & Conditions](#) and the [Ethical guidelines](#) still apply. In no event shall the Royal Society of Chemistry be held responsible for any errors or omissions in this *Accepted Manuscript* or any consequences arising from the use of any information it contains.

COMMUNICATION

Three-dimensionally designed Anti-reflective Silicon Surfaces for Perfect Absorption of Light†

Cite this: DOI: 10.1039/x0xx00000x

Seong J. Cho,^{ab} Taechang An,^{c*} and Geunbae Lim^{a*}

Received 00th January 2012,
Accepted 00th January 2012

DOI: 10.1039/x0xx00000x

www.rsc.org/

An ideal black material absorbs light perfectly over all wavelengths and is totally nonreflective. Material and structural design are crucial to the management of reflectivity. Here, we report a three-dimensionally designed (3D) silicon structure consisting of silicon pillars. To our knowledge, this 3D hierarchical surface has the lowest specular reflectance among silicon-based materials reported to date.

Solar energy has become the focus of increased attention over the past decade as fossil fuel resources diminish.¹ Devices such as solar cells, which are designed to convert sunlight into usable energy, are of particular interest.^{2–4} Light absorption is the one of the key factors that affect the conversion efficiency of solar cells.⁵ The sum of the transmission, reflection and absorption of the incident flux equals unity. Thus, reflectance and transmittance must be minimised to improve light absorption. A typical solar cell can prevent the transmittance of visible light through the silicon layer (silicon thickness: 180–300 μm). Thus, minimising reflectance remains a challenge. However, transmittance through thin-film-type solar cells is significant. Therefore, new trapping structures that use surface plasmons have received much attention.^{6,7}

The reflectance (R) at a flat interface is a function of the refractive index (RI). According to the Fresnel equation, $R = [(n_1 - n_2) / (n_1 + n_2)]^2$, where n_1 and n_2 are the RIs of the two media. Thus, the design of the RI profile is a major concern in developing an anti-reflective (AR) and highly absorbable surface. There have been many efforts to develop a new RI profile design that minimises the reflectance of a silicon substrate. The designs can be classified into two groups: (i) material and (ii) structural.

The typical material design inserts an AR coating layer having an intermediate RI, n_{AR} ($n_1 < n_{AR} < n_2$), between a silicon substrate and air. A variety of materials including silicon nitride,^{8,9} titanium dioxide^{10,11} and polymers¹² have been utilised as an AR layer. For example, a silicon nitride coating is the most industrially preferred for an AR layer because of its excellent surface passivation properties. Material design provides a limited tunability of the RI profile, resulting in relatively low AR performance (i.e. reflectance ca. 10%).¹³ To overcome the low performance, an advanced design

using a multi-layered coating with a graded refractive index has been reported.¹⁴

The structural design is also a significant factor affecting the RI. In the case of a sub-wavelength structure, the refractive index is determined not only by the intrinsic optical properties but also its volume fraction; i.e. the RI can be controlled by varying the composition of the structure. For example, porous silicon has RIs ranging from 1.1–3.2 depending on the volume fraction.¹⁵ Recently, a novel bio-inspired nanostructure that mimics the compound eyes of a moth has been reported. The configuration of a sub-wavelength array in the eyes generates a graded refractive index¹⁶ similar to an ideal RI profile because the volume fraction gradually changes. Consequently, the reflectance is reduced dramatically over a broad band of wavelengths regardless of the incident angle.¹⁷

Control of the light path also plays a crucial role in reducing reflectance. Microtexture that is greater than the wavelength of the incident light traps the light by multiple internal reflections. Various shapes of micro-AR surfaces, such as pyramidal¹⁸ and hemispherical¹⁹, have been studied. For example, a glass surface coated with silica microspheres diminished reflectance (7.6%) and increased transmittance (92.7%) over visible wavelengths because of the multiple internal reflections effect.¹⁹

Here, we report a three-dimensionally designed (3D) silicon structure consisting of cone-shaped micropillars and nanohairy structures. This structure was prepared using maskless plasma etching and self-assembly methods. Many previous AR approaches have focused on the fabrication of a simple and mono-scale structure such as a periodic nanopillar structure or a microtextured structure. A multi-layered and hierarchically designed structure enhances light absorption and carrier collection efficiency. Our micro-/nano-scale pillar structure not only generates an enhanced graded RI profile in every part of the surface but also strengthens the multiple internal reflections. Along with the unique morphology, we used a polyaniline (PANI) layer as an intermediate layer, which has a lower RI (1.29–1.63 in the UV-visible range²⁰) than silicon, to maximise anti-reflectivity. Consequently, the multi-layered and hierarchical structure showed near-ideal anti-reflectivity with specular reflection less than 0.01% (0.0031% at visible wavelengths) and a total reflectance of 0.5% in the UV-visible-NIR range (300–2000 nm). To our knowledge, the specular reflectance of 0.0031% is the lowest ever reported for silicon-based materials.¹⁷ Importantly, the anti-

reflective structure was fabricated using simple and economical self-assembly-based processes, and did not require accurate optics or high-temperature thermal processes.

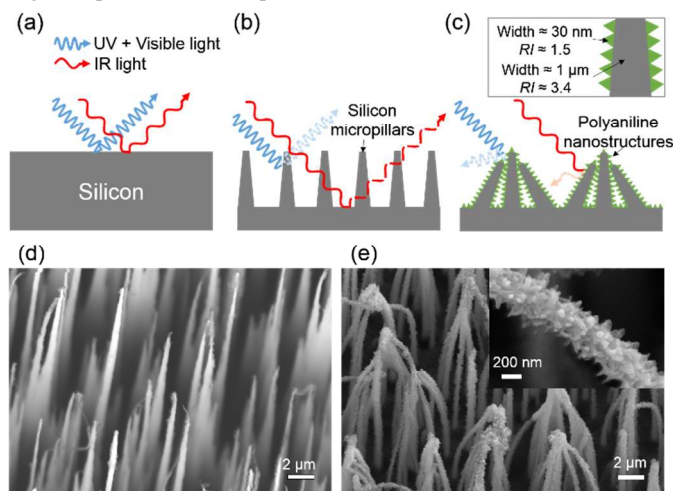
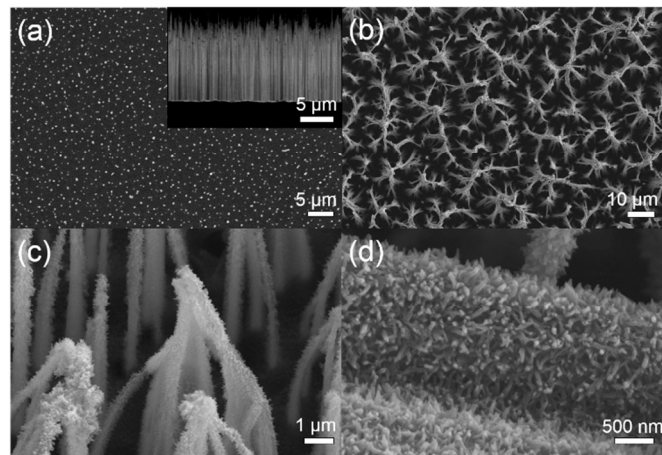


Fig. 1 Fabrication of a 3D hierarchical silicon surface consisting of high-aspect-ratio pillars and a sub-wavelength nanostructure. (a) Schematic diagram of reflection from a polished silicon surface showing strong reflection of UV and visible light from the flat surface. (b) 1D micropillar silicon surfaces made using DRIE and based on the “black silicon” method. The surface suppresses the reflection of most UV and visible light. (c) PANI-coated 3D hierarchical surface with a hairy nanostructure generated by a dilute polymerisation and capillary self-assembly process. The surface exhibited extremely low reflectance because of the unique hierarchical morphology. (d, e) SEM images of a 1D micropillar silicon surface and a 3D hierarchical surface, respectively. The inset to (e) shows the magnified image of a silicon micropillar with a PANI-coated nanostructure.

Figure 1 shows schematic diagrams of the 3D hierarchical silicon surface. Reflection and refraction of light occur at the interface of two different media. According to Fresnel’s equation, reflection is a function of the difference in the refractive indices.²¹ Silicon has a relatively high refractive index of 3.42 (crystalline),²² whereas air has the lowest refractive index of 1.00. A polished silicon surface has a discontinuous refractive index profile, resulting in high reflectance (Figure 1(a)).

A more complex structure is necessary to suppress reflectance. Here, we propose two strategies: (i) maximise internal reflection using a trapping structure such as a hierarchical structure, and (ii) increase interfacial absorption by generating a graded refractive index using a sub-wavelength structure. Hence, we fabricated a 3D silicon surface consisting of bundled micropillar and nanohairy structures.

A silicon surface textured with micropillars was formed by DRIE based on the “black silicon” method.^{23,24} With this method, residual micromasks are formed on the silicon surface.²⁵ The process did not require any pre-processes, including lithography, and enabled the production of nanostructures at high throughput and low cost. Also, various crystal structures of silicon, including single-crystalline, polycrystalline and amorphous silicon can be used with this method.²⁶ The maskless etched micropillars had a high aspect ratio with a length of ca. 20 μm and a width of ca. 1 μm and a tapered structure, which could generate a graded refractive index (Figure 1(d)). Previous work reported that a one-dimensionally structured micropillar silicon surface (1D micropillar surface) minimised reflectance over a wide range of wavelengths by controlling features of the architecture, such as its length and density.^{24,27} However, the 1D microtextured surface was sparsely populated with a between-pillar distance of 1–3 μm (Figures 1(d) and 2(a)). In the plan view, the 1D micropillar surface occupied a small fraction of the silicon surface and had limited anti-reflectivity. The experimental data



indicated that the pillar structures had excellent anti-reflectivity over

Fig. 2 SEM images of the micropillar structure and the self-assembled 3D hierarchical structure. (a) Plan and cross-sectional (inset) SEM views of the micropillar silicon surface. (b) SEM plan view of the 3D hierarchical structure. (c-d) Magnified SEM images of the 3D hierarchical structure

the UV–visible wavelengths but not in the IR range.

Figure 1(c) and (e) show the final 3D hierarchical silicon surface (3D hierarchical surface). To enhance anti-reflectivity, the 1D micro silicon structures were coated with PANI using a dilute polymerisation method to form a hairy nanostructure.^{28,29} The dilute polymerisation method is a simple and self-assembly method, which can be used to coat numerous surfaces, regardless of the material or morphology. All surfaces were completely coated to a thickness of ca. 200 nm. The nanostructure had a sub-wavelength architecture with diameters of 20–40 nm and a length of ca. 100 nm. (Figures 2(d) and S1 in ESI†) The sub-wavelength structure plays a similar role in the nanonipple array of a moth’s eye; i.e. to generate a tapered refractive index, resulting in minimising the reflectance of the interface.^{16,30}

Additionally, the nanostructured Si pillars self-assembled as the aqueous solution evaporated. During evaporation, tens of pillars bundled up and reorganised into a cone shape. The morphology of the self-assembled structure can be modified by controlling the design parameters such as surface tension and stiffness.³¹ This bundled pillar structure on the surface occupied a larger area than a structure comprising perpendicular pillars across a 1D micropillar surface (Figure 2(b)). The bundled pillars maintained their shape after drying by van der Waals forces. The unique architecture of the self-assembled pillar structure provided excellent anti-reflectivity in the broadband wavelength range (including IR) because the complex cone shape consisting of bundled micro-/nanopillars maximised the trapping of light.

The specular reflectance and total reflectance of a polished bare silicon surface, 1D micropillar surface, and 3D hierarchical surface were measured over the UV–visible–NIR range. Figure 3(a) is a graph of the specular reflectance as a function of wavelength of the three types of silicon surface; i.e. polished, 1D micropillar, and 3D micro/nano. The polished silicon surface had a relatively high specular reflectance in the UV–visible–NIR range. The polished silicon had an average specular reflectance of ca. 54, 35 and 31% in the UV (300–400 nm), visible (400–800 nm) and NIR (1200–2000 nm) ranges, respectively. The 1D micropillar surface dramatically reduced the specular reflectance over the entire wavelength range, with average specular reflectances of 0.0421, 0.0822, and 0.3197% over the same UV, visible, and NIR ranges, respectively. These specular reflectance results are in good agreement with previous

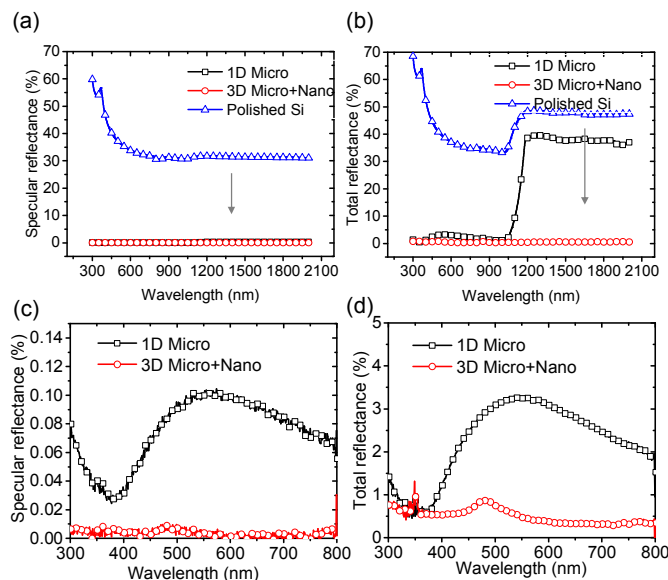


Fig. 3 Specular and total reflectances of polished, 1D pillar and 3D hierarchical surfaces as a function of wavelength from UV (300 nm) to the NIR (2000 nm). (a) Specular reflectance. (b) Total reflectance. The step increase at 1100 nm relates to the indirect band gap of silicon. (c) Expanded graph of (a) for the UV–visible range. (d) Expanded graph of (b) for the same range.

studies concerning nano- or micropillar silicon.^{17,32} For example, Huang et al. reported an anti-reflective Si surface with a specular reflectance of ca. 0.01% in the visible range.¹⁷ The 3D hierarchical surface had an extremely low reflectance, with average specular reflectances of 0.0046, 0.0031 and 0.0102% in the same UV, visible, and NIR ranges, respectively. To our knowledge, this 3D hierarchical surface has the lowest specular reflectance of silicon-based materials reported to date.

The 3D hierarchical surface also reduced the total reflectance. The polished bare silicon surface had a relatively high total reflectance in the UV and NIR ranges (Figure 3(b)). The average total reflectances in the UV, visible and NIR ranges were ca. 62, 39 and 48%, respectively. The increase in total reflectance beyond 1100 nm is related to the indirect band gap of silicon.³³ Additionally, the noisy reflectance at 350 nm in Figure 3(d) corresponds to changing of a source lamp. The total reflectance of the 1D micropillar surface was suppressed in the UV–visible–NIR ranges. In particular, the total reflectance in the UV and visible ranges was dramatically reduced to an order-of-magnitude lower than that of polished silicon; the average total reflectance decreased from ca. 62 to 1.2% in the UV range and 39 to 3.0% in the visible range. However, the reflectance in the NIR decreased only 10%, from 48 to 38%. This irregular reduction has been reported previously for 1D-structured Si surfaces.³³ The 3D hierarchical surface, on the other hand, exhibited excellent anti-total reflectivity (<1%) over the UV–visible–NIR ranges (Figure 3(b)). The surface had an average total reflectance of 0.6414, 0.4633 and 0.5215% in the UV, visible and NIR ranges, respectively. Table 1 summarises the specular and total reflectance for various Si surfaces. The 3D hierarchical surface reduced the specular reflectance to less than 10^{-4} that of the polished silicon surface in the UV and visible ranges.

The extremely low specular and total reflectances are related to the morphology of the 3D hierarchical surface, as noted previously. The cone-shaped micropillar clusters initially change the path of the incident light. The scattered light is reflected several times and becomes trapped in the 3D hierarchical structure. As the light path increases, so does the likelihood of the light being absorbed. However, a scattering effect could diminish the specular reflectance.

Table 1 Average specular and total reflectances in the UV–visible–NIR ranges.

	Specular reflectance (%)		
	Polished	1D Micro	3D Micro + nano
UV (300–400 nm)	54.0439	0.0421	0.0046
Visible (400–800 nm)	35.2259	0.0822	0.0031
NIR (1200–2000 nm)	31.3626	0.3197	0.0102
	Total reflectance (%)		
	Polished	1D Micro	3D Micro + nano
UV (300–400 nm)	61.5751	1.1842	0.6414
Visible (400–800 nm)	39.0719	2.9879	0.4633
NIR (1200–2000 nm)	48.0257	38.3085	0.5215

This explains the low specular reflection of the 3D hierarchical structure. The hierarchical structure also generated a near-ideal graded RI profile. The tapered micropillar structures (width: 100 nm (apex), 1 μm (base); length: 20 μm) generated a continuously graded RI profile.¹⁷ However, the dimensions of the microstructure were not sufficiently small to prevent all reflection and scattering. Only the apex of a silicon pillar had a sub-wavelength scale. To suppress reflection over a broad range of wavelengths, the surface structure must be reduced to the sub-wavelength scale. Our 3D hierarchical surface was covered with nanostructures having diameters of 20–40 nm, which are much smaller than the incident wavelengths (300–2000 nm). Conformal covering of nanostructures could prevent the reflection of scattered light as well as direct incident light.

The structured surface maintained its anti-reflectivity over a wide range of angles of incident light (Fig. S2, ESI†). The reflectance of the polished surface changed with the incident angle. The 1D micropillar surface and the 3D hierarchical surface maintained their anti-reflectivities regardless of the incident angle. Also, the surface exhibited excellent superhydrophobicity with a high water contact angle (CA) and low sliding angle (SA). The 3D hierarchical surface had a static CA of 179° and SA of < 1° (Fig. S3, ESI†). The improved anti-reflection properties and excellent anti-wetting properties of the surfaces could have extensive applications in renewable energy and electro-optical devices.

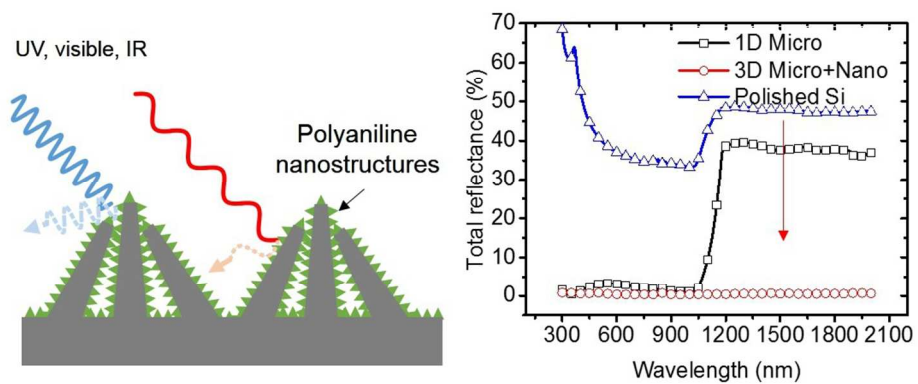
In summary, a novel 3D hierarchical silicon surface that consisted of high-aspect-ratio pillars and a sub-wavelength nanostructure was fabricated. The surface had near-ideal anti-reflection properties with an average specular reflection of < 0.01% (0.0031% at visible light wavelengths) and average total reflectance of ca. 0.5% over the UV–visible–NIR ranges. Moreover, the anti-reflective hierarchical structure was readily made using a maskless dry etching and a self-assembly process without invoking a nano-patterning process. Our facile fabrication approach for the 3D structure is an alternative strategy for production of a perfect anti-reflective surface and overcomes the shortcomings of current 1D-structured surfaces. Although the 3D surface had excellent anti-reflective properties, we believe that the hierarchical structures are not fully optimised. We anticipate further improved performance over a wide range of wavelengths with more complex shapes and hierarchical structures.

This work (2012R1A2A2A06047424) was supported by Mid-career Researcher Program through NRF grant funded by the MSIP

Notes and references

^a Department of Mechanical Engineering, Pohang University of Science and Technology (POSTECH), Pohang, 790-784, Republic of Korea.

- ^b Polymer Research Institute, Pohang University of Science and Technology (POSTECH), Pohang, 790-784, Republic of Korea.
- ^c Department of Mechanical Design Engineering, Andong National University, Andong, Korea.
- † Electronic Supplementary Information (ESI) available: Experimental details and optical images. See DOI: 10.1039/c000000x/
1. N. S. Lewis and D. G. Nocera, *Proc. Natl. Acad. Sci. U. S. A.*, 2006, **103**, 15729–35.
 2. M. D. Kelzenberg, S. W. Boettcher, J. a Petykiewicz, D. B. Turner-Evans, M. C. Putnam, E. L. Warren, J. M. Spurgeon, R. M. Briggs, N. S. Lewis, and H. a Atwater, *Nat. Mater.*, 2010, **9**, 239–44.
 3. Z. Fan, H. Razavi, J. Do, A. Moriwaki, O. Ergen, Y.-L. Chueh, P. W. Leu, J. C. Ho, T. Takahashi, L. a Reichertz, S. Neale, K. Yu, M. Wu, J. W. Ager, and A. Javey, *Nat. Mater.*, 2009, **8**, 648–53.
 4. F. Priolo, T. Gregorkiewicz, M. Galli, and T. F. Krauss, *Nat. Nanotechnol.*, 2014, **9**, 19–32.
 5. H. K. Raut, V. A. Ganesh, a. S. Nair, and S. Ramakrishna, *Energy Environ. Sci.*, 2011, **4**, 3779.
 6. S. Morawiec, M. J. Mendes, S. A. Filonovich, T. Mateus, S. Mirabella, H. Aguas, I. Ferreira, F. Simone, E. Fortunato, R. Martins, F. Priolo, and I. Crupi, *Opt. Express*, 2014, **22**, A1059–70.
 7. H. a Atwater and A. Polman, *Nat. Mater.*, 2010, **9**, 205–13.
 8. B. Sopori, *J. Electron. Mater.*, 2003, **32**, 1034–1042.
 9. H. Nagel, A. G. Aberle, and R. Hezel, *Prog. Photovoltaics Res. Appl.*, 1999, **7**, 245–260.
 10. C. Martinet, V. Paillard, A. Gagnaire, and J. Joseph, *J. Non. Cryst. Solids*, 1997, **216**, 77–82.
 11. J. Szlufcik, J. Majewski, A. Buczkowski, J. Radojewski, L. Jędral, and E. B. Radojewska, *Sol. Energy Mater.*, 1989, **18**, 241–252.
 12. J. Zhang, S. Shen, X. X. Dong, and L. S. Chen, *Opt. Express*, 2014, **22**, 1842–51.
 13. P. Doshi, G. Jellison, and A. Rohatgi, *Appl. Opt.*, 1997, **36**, 7826–37.
 14. J.-Q. Xi, M. F. Schubert, J. K. Kim, E. F. Schubert, M. Chen, S.-Y. Lin, W. Liu, and J. A. Smart, *Nat. Photonics*, 2007, **1**, 176.
 15. E. V. Astrova and V. A. Tolmachev, *Mater. Sci. Eng. B*, 2000, **69-70**, 142–148.
 16. P. B. CLAPHAM and M. C. HUTLEY, *Nature*, 1973, **244**, 281–282.
 17. Y.-F. Huang, S. Chattopadhyay, Y.-J. Jen, C.-Y. Peng, T.-A. Liu, Y.-K. Hsu, C.-L. Pan, H.-C. Lo, C.-H. Hsu, Y.-H. Chang, C.-S. Lee, K.-H. Chen, and L.-C. Chen, *Nat. Nanotechnol.*, 2007, **2**, 770–4.
 18. P. Papet, O. Nichiporuk, A. Kaminski, Y. Rozier, J. Kraiem, J.-F. Lelievre, A. Chaumartin, A. Fave, and M. Lemitte, *Sol. Energy Mater. Sol. Cells*, 2006, **90**, 2319–2328.
 19. Y. Wang, L. Chen, H. Yang, Q. Guo, W. Zhou, and M. Tao, *Sol. Energy Mater. Sol. Cells*, 2009, **93**, 85–91.
 20. D. Mo, Y. Lin, K. Gong, G. Zhang, and R. Yuan, *Chinese Phys. Lett.*, 1993, **10**, 374–376.
 21. S. Chattopadhyay, Y. F. Huang, Y. J. Jen, a. Ganguly, K. H. Chen, and L. C. Chen, *Mater. Sci. Eng. R Reports*, 2010, **69**, 1–35.
 22. M. Bass, C. DeCusatis, J. M. Enoch, V. Lakshminarayanan, G. Li, C. MacDonald, V. N. Mahajan, and E. Van Stryland, *Handbook of Optics, Third Edition Volume IV: Optical Properties of Materials, Nonlinear Optics, Quantum Optics (set)*, McGraw Hill Professional, 2009.
 23. H. Jansen, M. De Boer, R. Legtenberg, and M. Elwenspoek, *J. Micromechanics Microengineering*, 1995, **5**, 115–120.
 24. S. J. Cho, T. An, J. Y. Kim, J. Sung, and G. Lim, *Chem. Commun. (Camb.)*, 2011, **47**, 6108–10.
 25. M. Gharghi and S. Sivoththaman, *J. Vac. Sci. Technol. A Vacuum, Surfaces, Film.*, 2006, **24**, 723.
 26. S. Koynov, M. S. Brandt, and M. Stutzmann, *Appl. Phys. Lett.*, 2006, **88**, 203107.
 27. S. J. Cho, S. Y. Seok, J. Y. Kim, G. Lim, and H. Lim, *J. Nanomater.*, 2013, **2013**, 1–8.
 28. S. J. Cho, H. Nam, H. Ryu, and G. Lim, *Adv. Funct. Mater.*, 2013, **25**, 5577–5584.
 29. N.-R. Chiou, C. Lu, J. Guan, L. J. Lee, and A. J. Epstein, *Nat. Nanotechnol.*, 2007, **2**, 354–7.
 30. W.-L. Min, B. Jiang, and P. Jiang, *Adv. Mater.*, 2008, **20**, 3914–3918.
 31. B. Pokroy, S. H. Kang, L. Mahadevan, and J. Aizenberg, *Science*, 2009, **323**, 237–40.
 32. L. Sainiemi, V. Jokinen, A. Shah, M. Shpak, S. Aura, P. Suvanto, and S. Franssila, *Adv. Mater.*, 2011, **23**, 122–6.
 33. Y. Kanamori, M. Sasaki, and K. Hane, *Opt. Lett.*, 1999, **24**, 1422–4.



We successfully demonstrate a novel three-dimensionally designed (3D) silicon structure, which has the most advanced property in the previous anti-reflective materials.

198x81mm (150 x 150 DPI)